Universal valence bands for rocksalt-type compounds and their connection with those of tetrahedral crystals*

Sokrates T. Pantelides†
Department of Applied Physics, Stanford University, Stanford, California 94305
(Received 12 December 1974)

Using a limited tight-binding basis set, we obtain a universal set of analytical valence bands for rocksalt-type compounds and the rare-gas solids. The bands for each material are obtained by multiplying the universal bands by a scaling factor which is a simple function of the lattice constant and the chemical valence Z of the constituent atoms. Thus, in terms of only two empirically-determined parameters, we get complete valence bands for 51 crystals. We also obtain a universal density-of-states curve in terms of which photoemission spectra may be directly interpreted. Finally, we give a detailed comparison of the valence bands of rocksalt-type compounds with those of the zinc-blende-type compounds and show that the latter are a simple modification of the former. The only fundamental change is the introduction of a splitting at W, and along Z and Σ, which is a manifestation of the tetrahedral forces that are present in the zinc-blende but not the rocksalt crystals. This result complements the well-known fact that the zinc-blende bands are a simple modification of diamond-type bands.

I. INTRODUCTION

During the last ten years, the empirical pseudopotential method[1] (EPM) has very successfully given a complete picture of the energy bands of tetrahedrally bonded semiconductors.[2,3] The method did away with the most difficult problem of constructing the crystal potential and, instead, by employing a plane-wave basis set for the Bloch functions, it obtains values for the potential matrix elements by fitting to selected experimental data for the bands. Recently, it has been shown by a number of workers[4-6] that the valence bands of these materials may be equally well described by employing a tight-binding (TB) basis set and again obtaining values for the matrix elements by fitting to experimental data. We will refer to this as the empirical tight-binding method (ETBM). It has a particular advantage over the EPM in that it yields *analytical* expressions for the bands along symmetry lines, allowing a critical analysis of what determines the magnitude of particular eigenvalues, gaps, etc. In addition, Pantelides and Harrison[6] deduced rules governing the behavior of the TB parameters from material to material in terms of bond length and polarity[7] and successfully predicted valence bands for the entire class of the tetrahedrally bonded zinc-blende-type semiconductors.

Since the EPM has a *free-electron* starting point and the ETBM has a *free-atom* starting point, it is natural to expect the latter to be particularly suited for the more insulating, ionic crystals of rocksalt-type structure. In particular, we will consider the alkali halides, the alkaline-earth chalcogenides, and the less frequently studied monopnictides of Sc, Y, La, and the rare earths. As a special case we will also consider the rare-gas solids which crystallize in an fcc structure. This entire class of materials is clearly identified by rearranging the Periodic Table of the elements as we did in Ref. 6 (Fig. 1). The group-IV semiconductors C, Si, Ge, Sn, and the III-V, II-VI, and I-VII compounds are tetrahedrally coordinated and mostly (or entirely) covalently bonded.[8] On the other hand, the binary compounds formed from elements from the columns neighboring and straddling the rare gases, of interest here, are octahedrally coordinated, crystallize in the rocksalt structure and are primarily bonded via ionic Coulomb forces. (A few exceptions crystallize in the CsCl structure which is also close-packed ionic.) The rare earths behave in much the same manner as Sc, Y, and La, and form the rare-earth pnictides, which also crystallize in the rocksalt structure.

To be sure, many good calculations of the bands of many rocksalt-type compounds exist, in terms of TB or other basis sets, with one or another approximation to the crystal potential. What we want to show in this paper is that in terms of the ETBM we can obtain a universal set of valence bands for all such compounds.[9] In the end we will deduce the detailed valence bands and the total bandwidth of 51 such crystals. We also obtain a density-of-states curve and identify its various features with particular eigenvalues, a step that can help interpret x-ray photoemission (XPS) data in detail, in the manner so thoroughly carried out for the tetrahedral semiconductors.[2] Finally, we will

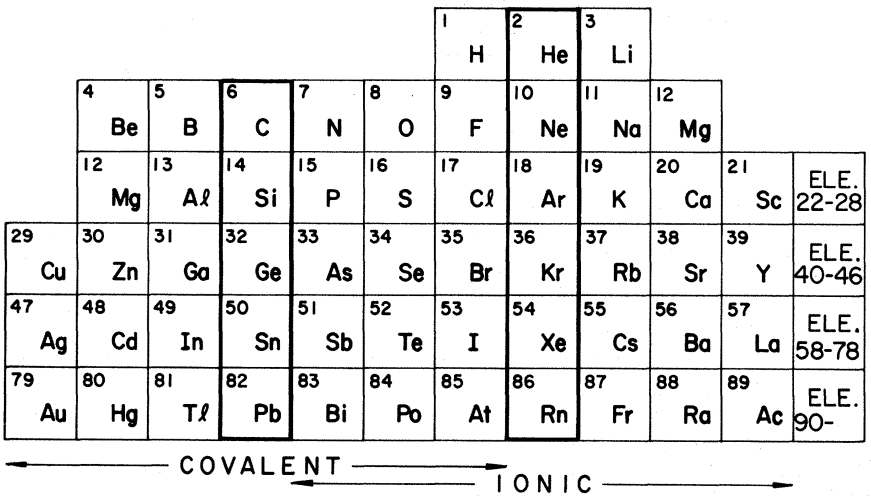

FIG. 1. Periodic Table of the elements rearranged in a fashion that is more appropriate for systematic studies of binary compounds. The compounds straddling the group-IV elements are covalent and tetrahedral (with four exceptions) and one can identify horizontal and skew isoelectronic series. On the other hand, the compounds straddling the rare-gas column are all ionic and crystallize in the NaCl or CsCl structures. Isoelectronic series, such as, for example, Kr-KCl-CaS-ScP, can again be identified. The compounds of Mg exist as both tetrahedral and ionic (Ref. 8) and this is shown by inserting Mg at two places in the Periodic Table. The rare earths not shown are elements 57–71. The other elements not shown are the three d periods of transition elements and actinides.

present a detailed comparison of the valence bands of the rocksalt-type compounds with those of the tatrahedral crystals and establish a connection between the two types of materials.

II. VALENCE BANDS OF ROCKSALT-TYPE CRYSTALS

We begin by choosing the limited TB basis set formed by the three orthogonal p orbitals on the negative nonmetallic anions of the NaCl-type compound. These ions form an fcc lattice. The resulting 3×3 Hamiltonian matrix $H_{\alpha\beta}(\vec{k})$ is real and can be diagonalized with the help of symmetry in the entire $k_x k_y$ plane to give

$$\lambda_1 = H_{33} , \tag{1}$$

$$\lambda_{2,3} = \tfrac{1}{2}(H_{11}+H_{22}) \pm [\tfrac{1}{2}(H_{11}-H_{22})^2 + H_{12}^2]^{1/2} . \tag{2}$$

Along the [111] direction we get

$$\Lambda_3 = H_{11} - H_{12} \text{ (doublet)} , \tag{3}$$

$$\Lambda_1 = H_{11} + 2H_{12} . \tag{4}$$

Explicit analytical expressions for the matrix elements $H_{\alpha\beta}(\vec{k})$ can be obtained by retaining only interactions between nearest-neighbor anions. These are expressed in terms of a p-bonding matrix element V_p and a π-bonding matrix element V_π as shown in Fig. 2 (The complete expressions are given in Appendix A.) At the points of high symmetry of particular interest one has

$$X_{5'} = -4(V_p - 3V_\pi) , \tag{5}$$

$$X_{4'} = -8(V_p - V_\pi) , \tag{6}$$

$$L_{3'} = -2(V_p - 5V_\pi) , \tag{7}$$

$$L_{2'} = -4(2V_p - V_\pi) , \tag{8}$$

where the zero of energy is taken at Γ_{15} (see Fig. 3 for notation). Similar expressions were obtained by early workers who attempted to compute values for V_p and V_π from first principles.[10] We shall not follow that route here.

First we wish to justify the approximations made thus far. This can be done by including next-nearest-neighbor anion interactions and also by expanding the basis set to include an s orbital on the metallic cations, which would generate the lowest conduction band.[11] When this procedure is carried out analytically, it is found that, by sym-

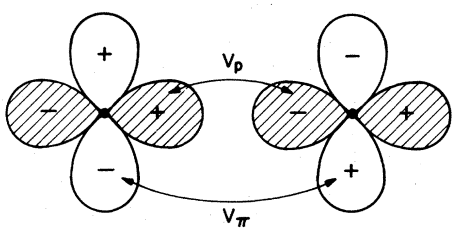

FIG. 2. Definition of the matrix elements V_p and V_π. Both are defined so that they are positive quantities. The p orbitals shown are located on nearest-neighbor anions so that the line connecting the two sites is in one of the [110] directions.

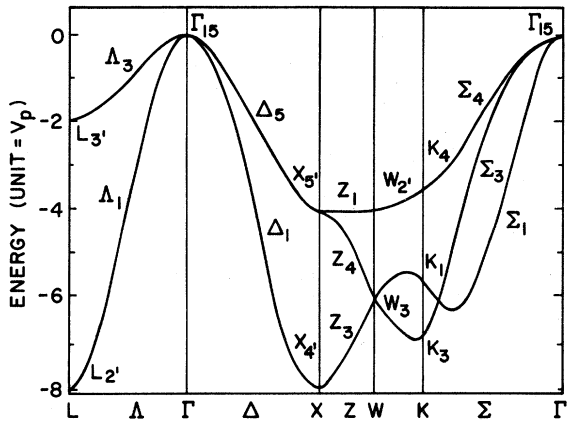

FIG. 3. Valence bands for rocksalt-type compounds when only the p-bonding matrix elements V_p between nearest-neighbor anions is retained. The unit of energy is V_p. For the symmetry notation the origin is taken at an anion.

metry, neither contribution alters the eigenvalues at Γ or X, but the eigenvalue $L_{2'}$, which represents the total bandwidth, is depressed in energy. Thus, by using (6) and (8), we can write

$$X_{4'} - L_{2'} = 4V_\pi + \text{correction} . \tag{9}$$

A survey of band calculations for these materials[12] shows that the quantity $X_{4'} - L_{2'}$ is in general very small, of order 10% of the total bandwidth. Thus, retaining only V_p and V_π is liable to introduce errors of about 0.1–0.2 eV in the valence bands, which is well within the limits of any experimental or theoretical determination of bands.

Next we turn our attention to the ratio of V_p and V_π. In view of (9) and the smallness of $X_{4'} - L_{2'}$, taking $V_\pi = 0$ would not be an unreasonable approximation. It would yield for the total width

$$L_{2'} = X_{4'} = 2X_{5'} = 4L_{3'} = 8V_p \tag{10}$$

and the over-all bands would still be quite good. They are shown along symmetry lines in Fig. 3.

A better description of the bands is of course obtained by retaining a nonzero value for V_π. Equation (7) shows that $V_\pi < \frac{1}{5}V_p$ if $L_{3'}$ is to lie below Γ_{15}. As was the case in tetrahedral compounds, we expect the ratio V_p/V_π to be independent of material. A survey of a variety of calculations[12] and interpretation of recent experimental data[13] suggest the relation $L_{2'} = 3X_{5'}$, which yields $V_\pi = \frac{1}{8}V_p$. Assuming this ratio, the valence bands are given in terms of only one parameter V_p. The total width is $7.5V_p$ and, by using V_p as the unit of energy, a set of universal valence bands for an arbitrary rocksalt-type solid is obtained. They are given analytically in the $k_x k_y$ plane by

$$\Sigma_3 = -1.75(2 - \cos x - \cos y) + 0.5(1 - \cos x \cos y) , \tag{11a}$$

$$\Sigma_{1,4} = -0.875(4 - \cos x - \cos y - 2\cos x \cos y) + 0.25(2 - \cos x - \cos y) \pm 1.125[(\cos x - \cos y)^2 + 4\sin^2 x \sin^2 y]^{1/2} , \tag{11b}$$

where $x = k_x d$, $y = k_y d$, and $2d$ is the lattice constant. The symmetry notation is that appropriate to the [110] axis. Along the [111] axis they are

$$\Lambda_3 = -0.375(1 - \cos 2x) , \tag{12a}$$

$$\Lambda_1 = -3.75(1 - \cos 2x) . \tag{12b}$$

These bands are shown in Fig. 4 together with the resulting density of states.[14] The origin of the structure in the density-of-states curve is explicitly identified so that experimental XPS spectra may be used to obtain valence band eigenvalues as it has been extensively done for tetrahedral crystals.

III. EMPIRICAL RULE FOR THE BANDWIDTHS

As a last step, which makes the ETBM a truly powerful technique, we show that one need not compute V_p or determine it experimentally (by measuring the total bandwidth) for each material in order to have the valence bands in terms of absolute energy units, such as eV. We are once more guided from the results of studies of tetrahedral crystals for which the nearest-neighbor bonding matrix element was found by Harrison and Ciraci[7] to have a simple d^{-2} dependence on bond length. Subsequently, Pantelides and Harrison[6] found other nearest-neighbor matrix elements to obey the same d^{-2} rule. Such a dependence of matrix elements on d may be understood in a variety of ways,[7] perhaps the most plausible being in terms of the virial theorem which scales potential energies with kinetic energies. For this reason, a useful way to write the d^{-2} dependence of a parameter V is, as suggested by Harrison[15]

$$V = \eta(\hbar^2 d^{-2}/m) , \tag{13}$$

where the constant η is dimensionless. In search of such relations in the ionic crystals we plot in Fig. 5 the log of the optical band gap E_g against $\ln d$. The solid lines have a slope of -2 which indicates the d^{-2} law is well obeyed:

$$E_g = \eta_g(\hbar^2 d^{-2}/m) . \tag{14}$$

We call the constant η_g the universal *band-gap index* and we note that it may be taken to be only

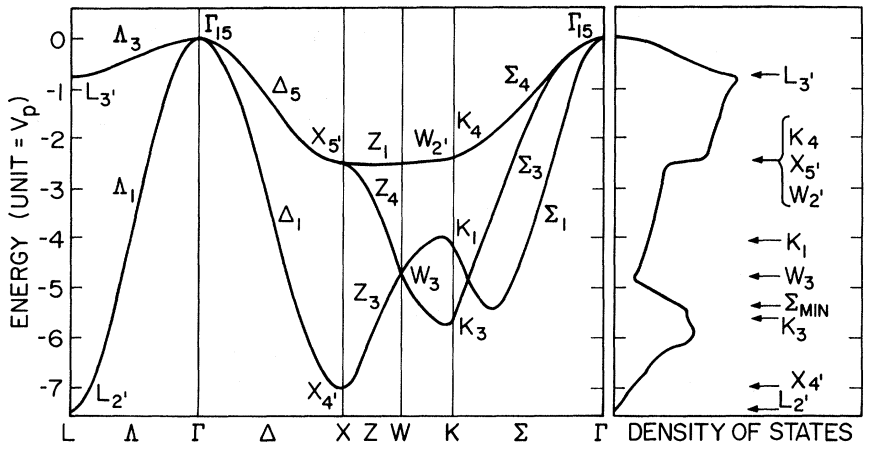

FIG. 4. Universal valence bands and density of states for rocksalt-type compounds in units of V_p.

a function of the chemical valence Z of the constituent atoms. We read the four values off Fig. 5 and list them in Table I along with the corresponding values of Z. We observe the following simple empirical relation

$$\eta_g = \eta_{g0} - 3.8Z \ , \tag{15}$$

where η_{g0} is the band-gap index for the rare-gas solids, equal to 12.9. We therefore proceed by assuming a d^{-2} law for V_p, or, equivalently the total bandwidth W_v,

$$W_v = 7.5\,V_p = \eta_v(\hbar^2 d^{-2}/m) \ , \tag{16}$$

where the universal *valence-band index* η_v is also taken to be a function of Z only. If this assumption holds, one needs to measure accurately the bandwidth of one material from each of the four classes ($Z = 0, 1, 2, 3$) in order to determine the four possible values of η_v. V_p and the complete valence bands for an arbitrary compound can then be determined by knowing its lattice constant alone.

Good XPS data exist for alkali halides[13] and some other compounds but none, to our knowledge, are available for any of the rare-earth pnictides. In order to predict the p valence bands for these materials as well, we assume, by analogy to (15), that η_v obeys the following simple relation:

$$\eta_v = \eta_{v0} + \alpha Z \ , \tag{17}$$

where η_{v0} is the valence-band index for the rare-gas solids. We fit the two unknown constants to η_v for the alkali halides as determined from the data of Pong and Smith[13,16] and to η_v for the chalcogenides as determined from a bandwidth of 7 eV for MgO.[17] This procedure yields $\alpha = 1$, whereby (17) reduces to the simple relation

$$\eta_v = \eta_{v0} + Z \ . \tag{18}$$

The resulting values of η_v are listed in Table II. Using these values we are then able to predict the total bandwidths for 51 crystals[18] as listed in Table II. We note that these predictions of band-

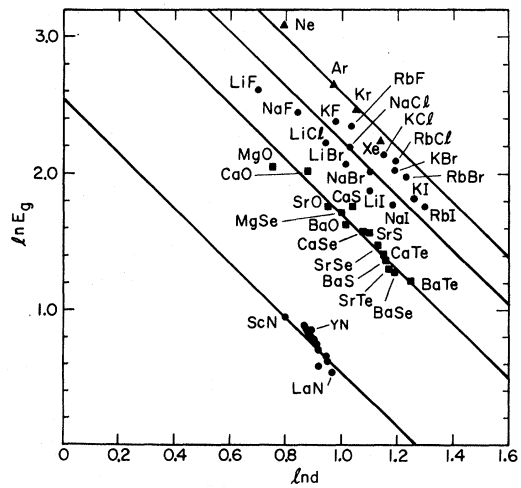

FIG. 5. Dependence of the optical band gap E_g on the lattice constant $2d$ for the rare-gas solids and rocksalt-type compounds. The unmarked circles are for the rare-earth nitrides. Other rare-earth pnictides are most likely to be semimetallic or metallic.

TABLE I. Universal band-gap index η_g and universal valence-band index η_v for the four classes of materials studied. All quantities are dimensionless.

Materials	Z	η_g	η_v
rare-gas solids	0	12.9	2.1
halides	1	9.1	3.1
chalcogenides	2	5.3	4.1
pnictides	3	1.6	5.1

widths do not depend on the ratio of V_p and V_π. The internal structure of the bands does. With the ratio assumed here, the complete valence bands in all cases are those of Fig. 4 in units of $\eta_v(\hbar^2 d^{-2}/m)$.

There are very few accurate experimental determinations of bandwidths for the rocksalt-type compounds which we can compare with our predictions of Table II. The recent XPS data of Kowalczyk *et al.*,[13] for the alkali halides are entirely consistent with our results. Bandwidths were not extracted from the data in Ref. 13 but comparisons can be made with the given spectra (Figs. 5 and 6 of Ref. 13). The agreement is excellent in the case of the three fluorides. For the compounds of the heavier anions the spectra show slightly wider bands which may be due to spin-orbit splittings. For example the spin-orbit splitting in atomic I is about 1 eV. Adding such a correction to our predicted bandwidths for the iodides yields very good agreement with the experimental spectra.

Our predictions are of course less reliable for the rare-gas solids and the nitrides for which the additional hypothesis (17) was employed. As for the d^{-2} assumption itself, it may not apply as well for the rare-gas solids in which the basis p orbitals are on neutral atoms instead of negative ions, whereby they are more tightly bound and their matrix elements may be influenced more by the chemical nature of the atom.

IV. COMPARISON WITH TETRAHEDRAL COMPOUNDS

A. Form of the bands

It is a well-known fact that the valence bands of the zinc-blende-type (zb) compounds are a modification of those of the diamond-type (dm) crystals, namely, the group-IV semiconductors diamond, Si, Ge, and α-Sn. The only fundamental modification of the over-all bands is the opening of a gap separating the three mostly-p-like bands from the mostly-s-like band at lower energies. From a physical point of view, a zb compound is constructed from a dm crystal by replacing each pair of identical atoms with a pair of dissimilar atoms. This eliminates the inversion symmetry and allows antisymmetric potentials, which manifest themselves by the introduction of the gap just mentioned. Hence this gap is often referred to as the "antisymmetric gap."

A zb compound may also be constructed by starting with a rocksalt-type (rs) compound. In this case one does not have to change the chemical identity of the constituent atoms but only their relative orientation. Hence many compounds, e.g., MgS, may be found in both structures. Take, for

TABLE II. Predicted valence-band widths W_v for the rare-gas solids and rocksalt-type compounds. Spin-orbit interactions have not been included. The lattice spacings ($2d$) are taken from Wyckoff, Ref. 8.

Z	Material	$2d$ (Å)	W_v (eV)
0	Ne	4.429	3.3
	Ar	5.256	2.3
	Kr	5.721	2.0
	Xe	6.197	1.7
1	LiF	4.017	5.9
	LiCl	5.130	3.6
	LiBr	5.501	3.1
	LiI	6.000	2.6
	NaF	4.620	4.4
	NaCl	5.628	3.0
	NaBr	5.973	2.7
	NaI	6.473	2.3
	KF	5.347	3.3
	KCl	6.293	2.4
	KBr	6.600	2.2
	KI	7.066	1.9
	RbF	5.640	3.0
	RbCl	6.581	2.2
	RbBr	6.854	2.0
	RbI	7.342	1.8
2	MgO	4.211	7.0
	MgS	5.203	4.6
	MgSe	5.451	4.2
	CaO	4.811	5.4
	CaS	5.690	3.9
	CaSe	5.910	3.6
	CaTe	6.345	3.1
	SrO	5.160	4.7
	SrS	6.020	3.5
	SrSe	6.230	3.2
	SrTe	6.470	3.0
	BaO	5.523	4.1
	BaS	6.388	3.1
	BaSe	6.600	2.9
	BaTe	6.986	2.6
3	ScN	4.440	7.9
	YN	4.877	6.5
	LaN	5.301	5.5
	CeN	5.011	6.2
	PrN	5.155	5.9
	NdN	5.151	5.9
	SmN	5.048	6.1
	EuN	5.014	6.2
	GdN	4.999	6.2
	TbN	4.933	6.4
	DyN	4.905	6.5
	HoN	4.874	6.5
	ErN	4.839	6.6
	TmN	4.809	6.7
	YbN	4.785	6.8
	LuN	4.766	6.8

example, MgS in the rs structure. The sulfur ions form an fcc lattice and the Mg-S dumbbell at each lattice is in the [100] direction (the magnesium ions also form an fcc lattice). If the dumbbells are now rotated to point in the [111] direction, the crystal becomes zb. Each set of ions still forms an fcc lattice by itself. Thus if we wish to describe the mostly-p-valence bands of zb MgS by using only a set of three p orbitals on the S's, as we did for the rs form of MgS earlier in this paper, we would get the same bands we got for the rs compounds, namely, Fig. 4. This, of course, may be an inadequate approximation, as we know from studies of tetrahedral compounds[5,6] and orbitals on the cations may have to be included. Thus, the valence bands of the zb compounds may be viewed as a modification of the rs valence bands, and any fundamental differences between the two must be due to the presence of tetrahedral forces which are present in the zb coordination but are not allowed in the octahedral rs coordination.

In Fig. 6 we show the p valence bands of a typical zb compound, GaAs, as calculated in the EPM by Chelikowski, Chadi, and Cohen.[2] (We have made some changes in the symmetry designation of some points which will be discussed in Sec. IV B.) The p valence bands we calculated for rs compounds in Sec. II are essentially identical to those of GaAs except for the region between the points X and K. In this region, the rs bands are shown in Fig. 6 as dashed lines. This demonstrates that the zb valence bands are indeed a modification of the rs bands. The fundamental difference between the two sets of bands is the splitting of the two lower bands at W and at the point along Σ where they used to cross in the rs case. As we remarked earlier, this must be due to the presence of tetrahedral forces and we designate it as the "tetrahedral splitting" in order to facilitate discussion. It is in many respects analogous to the "antisymmetric gap" introduced by antisymmetric potentials as one goes from dm to zb as discussed earlier. The term "splitting" is now more appropriate, however, instead of "tetrahedral gap" because the splitting does not introduce an absolute gap in the energy spectrum. (The "antisymmetric gap" can also in principle be reduced to an "antisymmetric splitting" if the L_1 eigenvalue were to be lowered in energy, below the X_1 eigenvalue of the s-like band.)

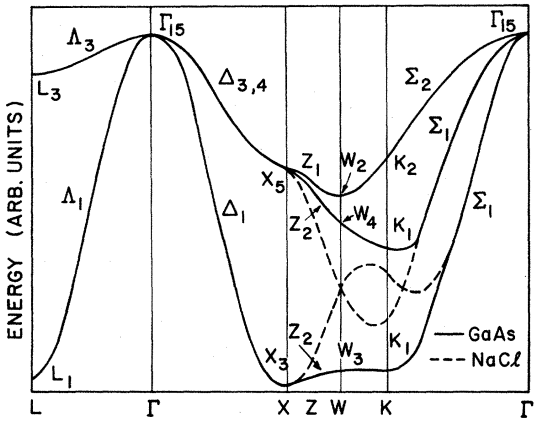

FIG. 6. Mostly-p-like valence bands of GaAs from Ref. 2 (solid lines). The dashed lines present the differences between the GaAs bands and the universal bands for rocksalt (NaCl)-type crystals determined in this paper (Fig. 4). At all other points the two sets of bands have negligible differences. Symmetry notation shown is that appropriate for GaAs with the origin taken at an As atom. Some of the labels, particularly at W, are different from those used in Ref. 2. See discussion in text how corrections were made.

B. Symmetry links

The effects we just discussed, namely, the appearance of the antisymmetric gap as one goes from dm to zb crystals and the appearance of the tetrahedral splitting as one goes from rs to zb crystals, may be described entirely in terms of group-theoretic considerations of the different symmetries.[19] All three types of crystals have an fcc Bravais lattice and thus they have the same Brillouin zone[20] (Fig. 7). They have different space groups, however, namely, O_h^7, O_h^5, and T_d^2 for dm, rs and zb crystals, respectively[21] (the rare-gas solids are indistinguishable from the rs

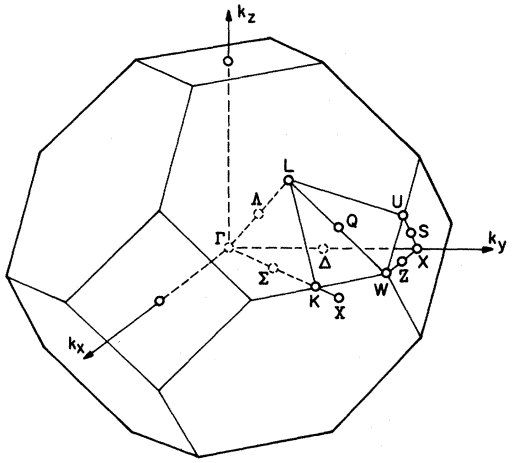

FIG. 7. Brillouin zone for fcc Bravais lattices appropriate for rare-ras solids, rocksalt-type compounds, zinc-blende-type compounds, and diamond-type crystals. The symmetry notation is that of Ref. 20.

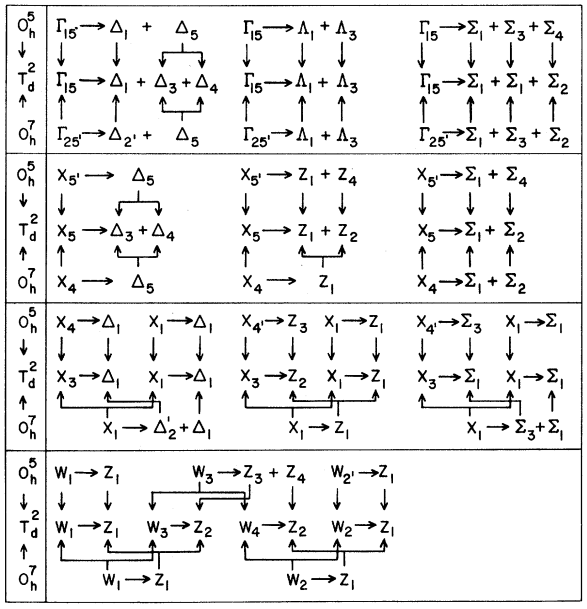

FIG. 8. Compatibility relations for each of the space groups O_h^5, T_d^2, and O_h^7 (horizontal arrows) and for going from O_h^5 to T_d^2 and also from O_h^7 to T_d^2 (vertical arrows). This schematic figure is constructed by combining several tables from Ref. 22.

crystals by means of symmetry). T_d^2 happens to be a subgroup of both O_h^7 and O_h^5. This means that a given irreducible representation of either O_h^7 or O_h^5 will go into one or more *specific* irreducible representations of T_d^2 when the appropriate symmetry operations are eliminated.[22] These are known as *compatibility relations*. All such relations that are used in this paper are given in schematic form in Fig. 8. The ones of interest at this point of the discussion are those represented by vertical arrows in Fig. 8. For example $\Gamma_{25'}$ of O_h^7 goes into Γ_{15} of T_d^2. Both of them are three dimensional. Similarly X_4 of O_h^7 goes into X_5 of T_d^2 and both are two dimensional. However, X_1 of O_h^7, which is two dimensional, goes into two one-dimensional representations, X_1 and X_3. Similarly W_1 goes into W_1 and W_3. This of course does not mean that X_1 and X_3 in a zb crystal cannot be accidentally degenerate. Only antisymmetric potentials can split them and thus the size of $\Delta X = X_3 - X_1$ is a measure of their strength.[23] Hence the designation antisymmetric gap, as noted in the beginning of this section.

Similarly, when one starts from O_h^5, Γ_{15} goes into Γ_{15}, $X_{5'}$ goes into X_5, etc. The important case here is that of W_3, which is a two dimensional representation in O_h^5, but goes into two one-dimensional representations, W_3 and W_4, in T_d^2. Finally, both the Σ_1 and Σ_3 rs bands, which cross each other (Fig. 4), go into Σ_1 in the zb crystals (Fig. 6). Again, all this does not mean that W_3 and W_4 cannot be accidentally degenerate, or that the two Σ_1 bands cannot accidentally be degenerate at a certain point and thus appear as crossing. In fact, we saw already, that this would be exactly the case if the p valence bands of zb crystals are described by employing only a set of three p orbitals on the anions. It is also clear that, if the basis set is enlarged, no anion-anion or cation-cation interactions can produce splitting. In other words, it is only *anion-cation interactions* which can differentiate the bands of the two crystal structures.[24] In rs crystals these interactions have the full O_h^5 symmetry of the fcc lattice (this is why the rare-gas solids have identical bands with the rs crystals), whereas in zb crystals they are tetrahedral. Thus the *magnitude* of the splitting at W and along Σ in the zb crystals is a measure of the *strength* of the anion-cation interactions, the only tetrahedral forces. Therefore we expect this *tetrahedral splitting* to be larger for the more covalent compounds, becoming largest in the completely covalent, group-IV dm crystals.[25] The quantitative aspects of this trend are of interest for the tetrahedral crystals themselves and we discuss them further in Appendix B. Here we wish to note that this trend is very analogous to the trend exhibited by the antisymmetric gap ΔX as we go from dm crystals to the more polar compounds. The two trends are, of course, "inverse" of one another and together they provide a line connecting the three classes of materials. This is illustrated[26] in Figs. 9 and 10.

Figure 9 serves an additional purpose in that it helps settle the matter of labeling eigenvalues at symmetry points and lines. In pursuing the group-theoretic analysis we just presented, we found that the labeling of some levels as given in the current literature, particularly the levels at W in the zb bands, is not in agreement with compatibility relations. In Fig. 9 we give the full labeling[27] which is consistent with *two* kinds of compatibility relations: Those that relate the symmetry points with the symmetry lines of each set of bands within itself (*horizontal* arrows in Fig. 8), and those which relate the symmetry points or lines between the dm and the zb bands and also between the rs and the zb bands (*vertical* arrows in Fig. 8). Using the latter kind allows one to start with the symmetry labels of the dm bands, which have been unambiguously given in the literature, and determine all the symmetry levels for the zb and, in turn, the rs bands in a unique and unambiguous way. The only requirement is that a choice of origin (at an anion or at a cation) be

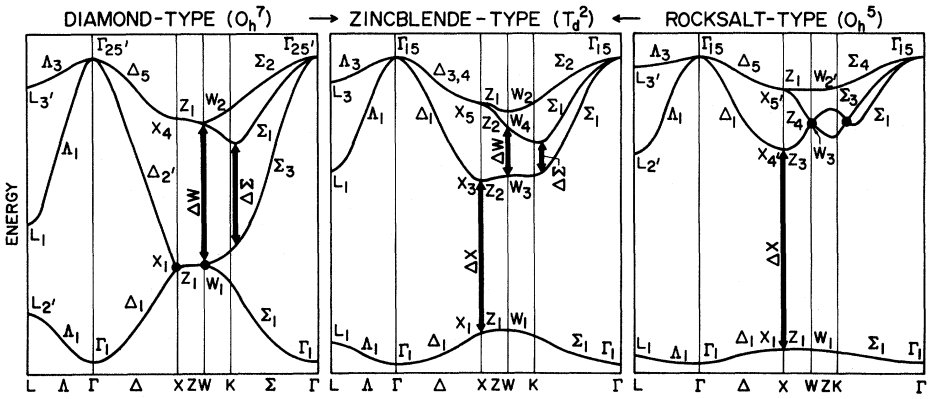

FIG. 9. Valence bands of a diamond-type material (first panel), zinc-blende-type material (second panel), and rocksalt-type material (third panel) used to illustrate the connections between the three sets of bands. For symmetry purposes the origin in the compounds is taken at an anion. Beginning with the first panel, notice the opening of the "antisymmetric gap" ΔX in the second and third panels. Beginning with the third panel, notice the opening of the "tetrahedral splittings" ΔW and $\Delta\Sigma$. See also Fig. 10.

made and maintained consistently. In this paper we choose the origin at an anion throughout.

C. Convergence rate of the ETBM

If we compare the results of Sec. III on the rs bands with the results of Refs. 5 and 6 which studied the dm and zb bands in the ETBM, it appears that there is a striking difference in the rate of convergence. In the case of the tetrahedral crystal, inclusion of only nearest-neighbor interactions has been known to yield extremely crude bands, with the top two bands being degenerate and flat throughout the Brillouin zone.[7] It has been found necessary to include π bonding in order to obtain curvature in the top two bands and also split them along the [110] direction.[4-6] This still did not give an adequate dip to the Σ_1 band and Chadi and Cohen[5] found that second-nearest-neighbor interactions (in terms of bond orbitals[6] this would be third neighbors) were needed to accomplish that and also to obtain dispersion along the Z symmetry axis. In contrast, in Sec. II we found that just one nonzero matrix element V_p is adequate to give us good over-all bands, dispersion along Z, and dip in the Σ_1 band, all without any π bonding. The inclusion of V_π and any other interactions do not change the bands substantially.

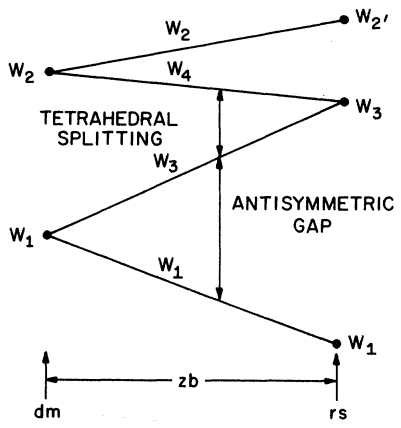

FIG. 10. Schematic illustration of the "antisymmetric gap" ΔX and the "tetrahedral splitting" ΔW in the diamond-type, zinc-blende-type, and rocksalt-type materials. Compare with Fig. 9.

Much of the apparent difference in the rate of convergence for the two sets of bands can be understood entirely in terms of the symmetry arguments given in Sec. IV B. For example, dispersion along the Z axis is inevitable in the rs bands, once the points X_5, and X_4, are not degenerate. This is because compatibility relations (Fig. 8) require X_5, to go into Z_1 and Z_4, and X_4, to go into Z_3; then Z_4 and Z_3 must merge together at W, to form a doublet, W_3. In contrast, symmetry does not guarantee dispersion along Z in the dm and zb bands.

On the other hand, if we examine more closely the type of matrix elements which enter in the two types of bands, the rates of convergence are entirely consistent with the discussion of Sec. IV B. In Ref. 6 it was found that the bands of tetrahedral compounds were obtained with very good accuracy at symmetry points by including only the interbond matrix elements B_1, B_4, and B_5. When these quantities were broken down into matrix elements of atomic orbitals on anions and cations these were found to correspond to nearest *anion-cation interactions* only. The magnitude of

these interactions, as we saw earlier, is determined by the tetrahedral forces and hence they are dominant in dm and zb crystals. Such anion-cation interactions are entirely negligible in the rs crystals (exactly zero in rare-gas solids) and never have to be considered. In these materials, the dominant interactions are *between anions*. Such anion-anion interactions were entirely neglected in Ref. 6 for tetrahedral materials. They are precisely the interactions invoked by Chadi and Cohen to reproduce dispersion along Z and a large enough dip in the Σ_1 band. We already saw that if only these anion-anion interactions are retained, neglecting the anion-cation nearest-neighbor interactions, one would get maximum dispersion along Z, maximum dip along Σ_1 and exactly the rs bands of Fig. 4. In a typical zb compound the anion-cation and the anion-anion effects on the Z and Σ bands tend to balance each other, the former prevailing in the completely covalent group-IV semiconductors and the latter prevailing in the more polar compounds. (See Appendix B.)

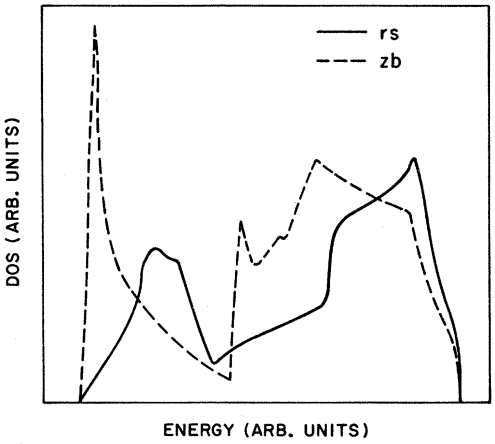

FIG. 11. Density-of-states curve for the rocksalt-type compounds obtained in this paper is compared with that of GaAs of Ref. 2. The total widths are taken the same but the ordinate scales are arbitrary. See discussion in text.

D. Densities of states

The differences in the bands just discussed naturally give rise to differences in the resulting density-of-states (DOS) curves. In Fig. 11 we superpose the universal DOS curve for rs materials determined in the present paper and the DOS curve for the p bands of GaAs from Ref. 2. The total widths were taken the same but the ordinate scales are arbitrary. We observe the following: They both have essentially a two-peak structure (especially, when rounded off by broadening); in both cases the dip coincides or is very near to a W eigenvalue. In fact, for the rs curve, the dip comes exactly at W_3 which lies at 0.63 of the total width below the top.[28] Concentrating on the structure of the peaks, we note that the low-energy peak is very tall and lopsided in the case of the zb curve. This appears to arise from the flat region along Z and W. This flat region is not present in the rs bands because the Z band must go up to meet the twofold W_3 as discussed earlier. The structures of the high-energy peaks are rather similar but also have distinct differences. We note that the little spike, present in the zb curve and due largely to the minimum in the Σ_1 band,[2] is absent in the rs curve because $\Sigma_{1\min}$ lies below the dip. Finally, the slope of the curve between the L and X critical points is reversed in the two materials. For the rs curve the L region appears to have a larger density of states than the X region. This is rather puzzling in view of Fig. 4, where X_5' is followed by a rather flat Z_1 band through to K_4. This means that understanding the *relative heights of peaks* in the DOS is not a task that can be completed entirely in terms of the shape of the bands along a few symmetry lines. The bulk of the zone is still the determining factor for the height of a peak resulting from a critical point.[29]

V. CONCLUSIONS

In conclusion, we have obtained a universal set of analytical valence bands for all rocksalt-type compounds and rare-gas solids. The valence bands for each material are obtained directly by multiplying the universal bands by a scaling factor which is a simple function of the lattice constant and the chemical valence of the constituent atoms. In terms of only two parameters we obtained complete valence bands for 51 crystals. We have also given a universal density-of-states curve in terms of which XPS data may be directly interpreted. Finally, we have presented a detailed comparison between the valence bands of the rocksalt-type compounds and those of the tetrahedral crystals, exploring some rather intricate relationships between the two sets of bands due to similarities and differences in symmetry.

ACKNOWLEDGMENT

I would like to express my thanks to Professor W. A. Harrison for many valuable discussions.

APPENDIX A: SECULAR MATRIX FOR THE ROCKSALT VALENCE BANDS

The 3×3 matrix $H(\vec{k})$ has the following matrix elements when only nearest-neighbor interactions are retained:

$$H_{11}=(V_p-V_\pi)[\cos(x+y)+\cos(x-y)+\cos(x+z)+\cos(x-z)]-2V_\pi[\cos(y+z)+\cos(y-z)]\ ,$$

$$H_{22}=(V_p-V_\pi)[\cos(y+z)+\cos(y-z)+\cos(y+x)+\cos(y-x)]-2V_\pi[\cos(x+z)+\cos(x-z)]\ ,$$

$$H_{33}=(V_p-V_\pi)[\cos(z+x)+\cos(z-x)+\cos(z+y)+\cos(z-y)]-2V_\pi[\cos(x+y)+\cos(x-y)]\ ,$$

$$H_{12}=(V_p+V_\pi)[\cos(x+y)-\cos(x-y)]\ ,$$

$$H_{13}=(V_p+V_\pi)[\cos(x+z)-\cos(x-z)]\ ,$$

$$H_{23}=(V_p+V_\pi)[\cos(y+z)-\cos(y-z)]\ .$$

Here x, y, z stand for k_xd, k_yd, and k_zd, respectively.

When an s orbital on the cations is added to the basis set, the result is a 4×4 Hermitian matrix. The 3×3 submatrix remains unchanged. Retaining nearest-neighbor interactions once more, the new matrix elements are given by

$$H_{44}=\epsilon_s-2V_{ss}[\cos(x+y)+\cos(x-y)+\cos(y+z)+\cos(y-z)+\cos(x+z)+\cos(x-z)]\ ,$$

$$H_{14}=-2iV_{sp}\sin x\ ,$$

$$H_{24}=-2iV_{sp}\sin y\ ,$$

$$H_{34}=-2iV_{sp}\sin z\ ,$$

where x, y, and z are as before and i is the imaginary unit. Analytical eigenvalues are again obtainable along symmetry lines.

APPENDIX B: QUANTITATIVE ASPECTS OF THE "TETRAHEDRAL SPLITTING" IN TETRAHEDRAL CRYSTALS

As noted in Sec. IV, the tetrahedral splitting is expected to be largest for the group-IV materials and progressively get smaller for the polar zinc-blende compounds. In Ref. 6 this kind of trends were predicted directly by breaking up the bond orbitals into hybrid orbitals whereby the polarity entered in a natural way. For example, the prediction was made that the splitting $\Gamma_{15}-X_5$ is largest for the group-IV materials (its symmetry notation in that case is $\Gamma_{25'}-X_4$) and progressively gets smaller according to the formula

$$\Gamma_{15}-X_5=(\Gamma_{25'}-X_4)_{\mathrm{IV}}\alpha_c\ , \tag{B1}$$

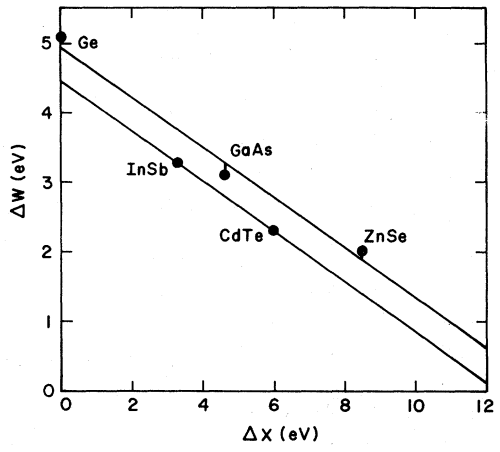

FIG. 12. Verification of the quantitative relationship between the tetrahedral splitting ΔW and the antisymmetric gap ΔX using the theoretical values of Ref. 2.

where α_c, the covalency,[7] is the complement of the polarity α_p so that $\alpha_c=(1-\alpha_p^2)^{1/2}$. Unfortunately, the eigenvalues at W and along Σ are not obtainable analytically for the zinc-blende crystals, in the manner done for other symmetry points and lines in Ref. 6. Analytical solutions are possible for the group-IV materials, however, and the result is

$$W_2=X_4\ (\text{doublet})\ , \tag{B2a}$$

$$W_1=X_1\ (\text{doublet})\ , \tag{B2b}$$

which means no dispersion along Z, as pointed out in Ref. 5. In the theory of Ref. 6, the only new matrix element that arises from antisymmetric potentials is B_1^a. This matrix element scrambles W_2 and W_1 into four levels (W_1, W_2, W_3, and

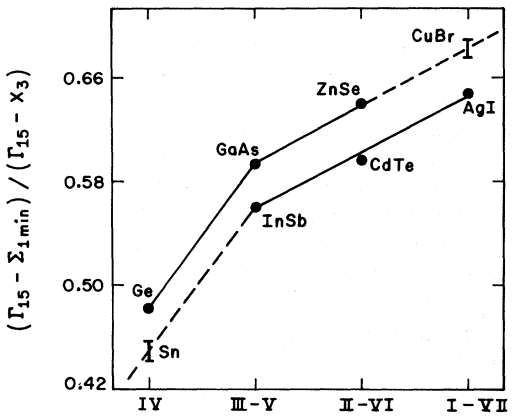

FIG. 13. Verification of the prediction that the dip in the Σ_1 band is larger for polar materials, when measured relative to the total width of the p bands. See text.

W_4; see Fig. 9) but to a good approximation we can first ignore the mixing between the two doublets of Eqs. (B2) and concentrate on $W_2 \rightarrow W_2 + W_4$ and $W_1 \rightarrow W_1 + W_3$. We can then add the additional coupling as a perturbation. The net result is

$$\Delta W = \Delta W_{\mathrm{IV}} - 8\lambda B_1^a \ , \tag{B3}$$

where ΔW is identified in Fig. 9 and λ is a numerical constant whose precise value is of no interest. The expression for B_1^a is[6]

$$B_1^a = \tfrac{1}{2}(\alpha_p V_1^s + V_1^a), \tag{B4}$$

whereby the variation of ΔW with polarity is more complicated than that of $\Gamma_{15} - X_5$ in Eq. (B1). Nevertheless, we recall that the antisymmetric gap ΔX is given by[6]

$$\Delta X = 8B_1^a \ , \tag{B5}$$

whereby (B3) becomes

$$\Delta W = \Delta W_{\mathrm{IV}} - \lambda \Delta X \ . \tag{B6}$$

This is a quantitative expression linking the antisymmetric gap ΔX with the tetrahedral splitting ΔW, a fact discussed qualitatively in Sec. IV and illustrated in Figs. 9 and 10. As was true with (B1) in Ref. 6, Eq. (B6) is guaranteed to be satisfied by the numerical results obtained for 39 tetrahedral in Ref. 6. (The eigenvalues at W were not listed in Ref. 6.) As an independent test, in Fig. 12 we plot the ΔW's against the ΔX's calculated by the EPM in Ref. 2 and we see that (B6) is well verified with the same λ for both isoelectronic sequences.

Another measure of the tetrahedral splitting is the splitting $\Delta\Sigma$ at $\Sigma_{1\,\mathrm{min}}$. Analytical expressions are even more difficult in this case, however. Nevertheless, a smaller $\Delta\Sigma$ implies a larger dip in the higher-energy Σ_1 band, *relative to the total width of the p bands* as measured by X_3. This is illustrated to be so in Fig. 13 where the experimental data of Ref. 30 were used.

Note added in proof. Further analysis showed that the dependence of the η's on Z is actually a dependence on *cation*. Cations with the same Z tend to have approximately the same η. See, for example, Fig. 5 where all compounds of cations with $Z = 2$ fall on the same line. The same is roughly true of the alkali halides ($Z = 1$), but four lines, one for each cation, each with slope -2, fit the data points slightly better. This distinction does not affect the results of this paper [except perhaps by introducing a small correction in Eqs. (15) and (18)] but has interesting consequences in other matters, e.g., the determination of dielectric constants (S. T. Pantelides, to be published). The theoretical basis for this dependence as well as the inclusion of spin-orbit interaction will be discussed at length elsewhere. Photoemission data on the valence bands of the rare-gas solids have recently been published by N. Schwenter *et al.* [Phys. Rev. Lett. 34, 528 (1975)]. Our predictions for the bandwidths agree very well with the experimental values for Xe and Kr, when allowance for spin-orbit effects is made, and less so for Ar and Ne, indicating that the d^{-2} rule is not well obeyed for the rare-gas solids. The universal valence bands described in this paper also apply to the compounds of antifluorite structure, such as Li_2O, Mg_2Si, etc. The valence bands of compounds with fluorite structure, such as CaF_2, are obtainable directly in terms of the bands described here and will be given elsewhere. Thus one obtains systematic connections between the bands of six classes of materials: rare-gas solids, rocksalt-type compounds, zinc-blende-type compounds, diamond-type crystals, fluorite-type compounds, and antifluorite-type compounds.

---

*Work supported by the National Science Foundation Grant No. GH-39811.

†Present address: IBM T. J. Watson Research Center, Yorktown Heights, New York 10598.

[1]M. L. Cohen and V. Heine, Solid State Phys. 24, 38 (1970).

[2]J. Chelikowsky, D. J. Chadi, and M. L. Cohen, Phys. Rev. B 8, 2786 (1973).

[3]J. C. Phillips and K. C. Pandey, Phys. Rev. Lett. 30, 787 (1973).

[4]N. J. Shevchik, J. Tejeda, and M. Cardona, Phys. Rev. B 9, 2627 (1974).

[5]D. J. Chadi and M. L. Cohen, Phys. Status Solidi (to be published).

[6]S. T. Pantelides and W. A. Harrison, Bull. Am. Phys. Soc. 20, 29 (1975); Phys. Rev. B. 11, 3006 (1975).

[7]W. A. Harrison, Phys. Rev. B 8, 4487 (1973); W. A. Harrison and S. Ciraci, *ibid.* 10, 1516 (1974).

[8]AgF, AgCl, and AgBr are exceptions; they crystallize in the rocksalt structure. The magnesium compounds are also of special interest: MgO is in the rocksalt structure at room temperature and pressure (RTP), MgS is stable in both rocksalt and zinc-blende structures, MgSe is in the zinc-blende structure at RTP but can very easily be converted to the rocksalt form, and finally, MgTe is known only in the zinc-blende structure [R. W. G. Wyckoff, *Crystal Structures* (Interscience, New York, 1965), Vol. 1, pp. 85–111]. Consistent with this is the observation that Mg may be allotted either to the zinc column (and hence the tet-

rahedral family) or the calcium column (and hence the rocksalt family).

[9]In this paper we do not consider rocksalt-type binary compounds of the transition metals. All the results obtained here will also apply for the p bands of those such compounds for which p-d hybridization is not strong.

[10]W. Shockley, Phys. Rev. 50, 754 (1936); R. C. Casella, *ibid.* 104, 1260 (1956); A. B. Kunz and W. J. Van Sciver, *ibid.* 142 (1966).

[11]The restriction of the basis set to only three p-like orbitals on the anions is not an approximation at all if the orbitals are thought of as the Wannier functions of the three valence bands. In that sense, Eqs. (1)–(4) are exact, and the only approximation is made in expressing the matrix elements $H_{\alpha\beta}(\vec{k})$ in terms of nearest-neighbor interactions alone. The Wannier-function concept also provides a rigorous justification for taking the p orbitals on nearest neighbors to be orthogonal.

[12]e.g., A. B. Kunz, J. Phys. C 3, 1542 (1970); A. B. Kunz and N. O. Lipari, J. Phys. Chem. Solids 32, 1141 (1971); Phys. Rev. B 4, 1374 (1971); F. Perrot, Phys. Status Solidi 52, 163 (1972); S. T. Pantelides, D. J. Mickish, and A. B. Kunz, Phys. Rev. B 10, 5203 (1974).

[13]W. Pong and J. A. Smith, Phys. Rev. B 9, 2674 (1974); S. P. Kowalczyk, F. R. McFeely, L. Ley, R. A. Pollak, and D. A. Shirley, *ibid.* 9, 3573 (1974).

[14]I am indebted to Professor M. L. Cohen and his group for supplying me with a copy of their program to compute densities of states. The method used is that of G. Gilat and L. J. Raunbenheimer, Phys. Rev. 144, 390 (1966).

[15]W. A. Harrison (private communication).

[16]The data for NaCl and KCl were used. The same value of $\eta_b(0.41)$ satisfied Eq. (16) for both materials, within the experimental uncertainty. The data for LiCl are less reliable according to the authors of Ref. 13 because the crystals are very hygroscopic.

[17]D. W. Fischer, Adv. x-Ray Anal. 13, 159 (1970); The value 7 eV is in agreement with the latest theoretical determination of the bandwidth by Pantelides *et al.*, Ref. 12.

[18]For the rare-earth nitrides the p band lies immediately above the f band and hybridization is possible. For the compounds of the heavy anions, spin-orbit interactions, not included in the present study, may be responsible for a larger bandwidth than determined here.

[19]The group-theoretic origins of the antisymmetric gap are well known. We repeat that discussion here for completeness and in order to bring out the full analogy between it and the tetrahedral splitting.

[20]L. P. Bouckaert, R. Smoluchowksi, and E. Wigner, Phys. Rev. 50, 58 (1936).

[21]J. C. Slater, *Quantum Theory of Molecules and Solids* (McGraw-Hill, New York, 1965), Vol. 2, p. 368.

[22]R. H. Parmenter, Phys. Rev. 100, 573 (1955).

[23]As shown in Ref. 6, the size of the antisymmetric gap $X_3 - X_1$ is not entirely determined by the antisymmetric potential but by the symmetric potential as well. Its dependence on the two kinds of potentials is such that the gap goes to zero when the antisymmetric potential is zero.

[24]D. J. Chadi, M. L. Cohen, and W. D. Grobman [Phys. Rev. B 8, 5587 (1973)] deduced from their pseudopotential that the antisymmetric gap ΔX becomes equal for zinc-blende and rocksalt compounds when V_{cation} goes to zero. We conclude here that the bands in their entirety become identical in the two kinds of compounds since both reduce to an fcc lattice of anions.

[25]The tetrahedral splitting remains finite in all tetrahedral compounds. Otherwise, in the absence of tetrahedral forces, the crystal would collapse in a rocksalt structure. Note that the vanishing tetrahedral splitting in the rs bands signifies the absence of tetrahedral forces but not necessarily the vanishing of anion-cation interactions.

[26]In the third panel of Fig. 9 we also show the s-like band below the p-like bands. This is generally classified as a core state (of the anion) and is essentially flat. Its energy separation from the top of the p bands is in most rocksalt crystals roughly 11–14 eV [see Kowalczyk *et al.*, Ref. 13; and S. T. Pantelides, Phys. Rev. B 11, 2391 (1975)], the same as in the zinc-blende compounds. Exceptions are the fluorides and the oxides in which the energy separation is 20–26 eV, the same as in the nitrides, oxides, and fluorides of zinc-blende coordination (Ref. 6).

[27]In addition to the W eigenvalue labels, another correction made in labeling the bands of zb crystals is the designation of the upper bands along Δ as Δ_3 and Δ_4 instead of Δ_5, which has been used in much of the literature. T_d^2 does not have a Δ_5 representation and in fact does not have a two-dimensional representation (Ref. 22). The two bands Δ_3 and Δ_4, however, "stick together" because of time-reversal symmetry (Ref. 22). They split when spin is included.

[28]This is true when V_π is taken equal to $V_p/8$ as done here. Thus, accurate determinations of the position of the dip from XPS data would either supply proof for this assumption, or help establish the precise ratio of V_π/V_p in each material. One can easily show that the position of the dip (W_3) relative to the total width W_v is given by $W_3/W_v = [3 - 5(V_\pi/V_p)]/[4 - 2(V_\pi/V_p)]$. The possible values of this ratio (allowed by the range $V_\pi = 0$ to $V_\pi = V_p/5$) is 0.56 to 0.75.

[29]A typical example of how the appearance of bands along symmetry lines may be misleading is the DOS for germanium, Fig. 2 of Ref. 2. The DOS goes through a minimum, almost zero, at the X_1 and W_1 points, where the bands appear flat. (See also Fig. 9, this paper.) On the other hand, there is a peak at $L_{2'}$ where the bands don't appear to be as flat.

[30]D. E. Eastman, W. D. Grobman, J. L. Freeouf, and M. Erbudak, Phys. Rev. B 9, 3473 (1974).